Experiments on the Interaction of Light and Sound for the Advanced Laboratory

D. T. PIERCE*
R. L. BYER
Applied Physics Department
Stanford University
Stanford, California 94305
(Received 12 June 1972; revised 10 October 1972)

We describe an advanced laboratory experiment in which both Raman–Nath and Bragg diffraction of light by acoustic waves in water are observed in the sound frequency range from 5 to 45 MHz. The apparatus consists of a laser, light detector, rf power source, quartz transducer, and homemade water cell. We discuss the theory of Raman–Nath diffraction, Bragg diffraction, and the criteria for the manifestation of each. The measured Raman–Nath diffracted orders give a visual display of FM sidebands. We discuss a quantitative relationship between the incident and diffracted light and the sound for Bragg diffraction in terms of a three-wave parametric process. Stanford students in the Advanced Applied Physics Laboratory have successfully performed this experiment during the past three years.

I. INTRODUCTION

The interaction of light and sound exhibits many interesting and useful effects. Sound waves can deflect light, change its frequency, and modulate its phase and amplitude. In turn the diffracted light can probe the spatial distribution of acoustic energy in the sound beam and give information on the velocity and attenuation of the sound wave and the elastic properties of the material.

All of these phenomena are dramatically observed in the laboratory experiment we describe here. A minimum of equipment is required: a HeNe laser, an rf power source, a light detector, a quartz crystal transducer, and a homemade water cell. This experiment has been well received in a graduate laboratory taught at Stanford which draws students from physics, applied physics, and electrical engineering. We believe that this experiment would also be suitable for a senior laboratory.

In 1922 Brillouin[1] presented a theory of light scattering from thermally excited elastic waves. He predicted that light would be diffracted by elastic waves in solids and liquids at the Bragg angle α given by $\sin\alpha=\lambda/2\Lambda$, where λ and Λ are the wavelengths of light and sound in the medium. The diffuse scattering of x rays has been extensively studied to determine thermal phonon distributions and the elastic constants of crystals.[2,3] In 1932 Debye and Sears[4] in the United States and, independently, Lucas and Biquard[5] in France first observed the diffraction of light by artifically generated elastic waves. These early experiments showed diffraction into several higher orders and a distribution of intensity in the higher orders that could not be explained by ordinary Bragg diffraction. A few years later Raman and Nath[6–10] in a series of papers developed a theory which explained the experimental observations.[11]

The interaction of light and sound displays different characteristics depending on the width of the interaction region, the light and sound wavelengths, and the amplitude of the sound wave. Roughly speaking, if the width, frequency, and amplitude of the sound beam are sufficiently small, the observed diffraction is explained by the theory of Raman and Nath and frequently is referred to as Raman–Nath diffraction. Conversely, Bragg diffraction is observed if the width, frequency, and amplitude of the sound beam are sufficiently large. We discuss quantitative criteria for these two types of diffraction in Sec. II. In Sec. II.A we discuss the Raman–Nath theory, which shows that the acoustic beam can be treated as a phase grating which modulates the light similar to FM wave modulation. A powerful approach to the interaction of light and sound in the Bragg regime is to treat it as a three-wave

parametric process.[12] Our discussion of this approach to Bragg diffraction in Sec. II.B is of interest since other phenomena such as optical parametric oscillation, Brillouin scattering, and Raman scattering can be treated analogously. The Bragg angle condition and the frequency shift of the light results naturally from conservation of energy and momentum when treated as a parametric process.

In this experiment we explore the diffraction of light from traveling waves in a liquid over the wide range from Raman–Nath to Bragg diffraction. The somewhat related recent article by Kang and Young[13] discusses Raman–Nath diffraction from standing waves with particular emphasis on determining the length of the sound wave and understanding the physical optics behind the striation pattern observed in the Schlieren method.

In Sec. III we discuss the apparatus used in our laboratory experiment and the observed Raman–Nath and Bragg diffraction results. The ultrasonic wave is conveniently generated in water which diffracts light very efficiently. The full range of Raman–Nath and Bragg diffraction is observed in the acoustical frequency range of 5 to 45 MHz. The use of a HeNe laser with its monochromatic, well collimated beam greatly facilitates the experiment.

The development of the laser and improvements in acoustical techniques, particularly in the microwave region, have generated renewed interest in the interaction of light and sound and have rendered feasible new applications and the observation of new phenomena. Many of the applications rest directly on the basic experimental results of Sec. III while others require some extensions of these experiments.

II. THEORY

A. Raman–Nath Diffraction

Figure 1 shows the essentials of the Raman–Nath diffraction where a light wave with wave vector $\mathbf{k}$, frequency ω, and wavelength λ in the medium is incident parallel to the wavefronts of a traveling sound wave characterized by $\mathbf{k}_s$, ω_s, and wavelength Λ. At any instant in time the sound wave creates alternate regions of compression and expansion, periodic variations in density

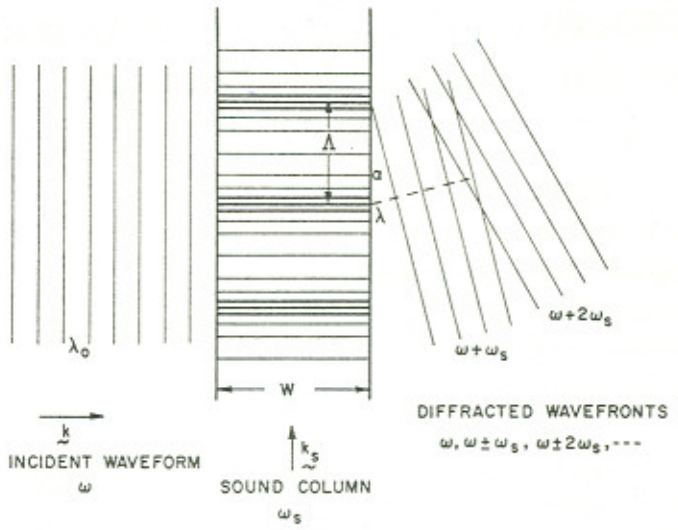

FIG. 1. Schematic drawing of Raman–Nath diffraction. Light incident on the sound column of width W, frequency ω_s, and wavelength Λ is diffracted at frequencies $\omega\pm\omega_s$, $\omega\pm2\omega_s$, etc., and approximate angles λ/Λ, $2\lambda/\Lambda$, etc.

which produce a periodic variation in the refractive index. To introduce the Raman–Nath theory we assume that the width W of the sound wave is small enough so that curvature of the light rays is negligible. Only the velocity and therefore the phase of the light changes with the variation of the refractive index. The light wave emerges from the sound wave with its amplitude constant but its phase a periodic function of position with a period Λ. Hence the sound wave acts like a phase grating. The change in phase $\Delta\phi$ of a light wave passing through a region where the normal refractive index n is changed by Δn is given by

$$\Delta\phi = W\Delta k = W(\omega/c)(n+\Delta n) - (W\omega n/c)$$
$$= 2\pi W\Delta n/\lambda_0, \qquad (1)$$

where λ_0 is the light wavelength in a vacuum. The change in the refractive index is related to the change in density by $\Delta n/n = \Delta\rho/\rho$. The sound power density P_s is given by[14]

$$P_s = \rho\tfrac{1}{2}v^3(\Delta\rho/\rho)^2 = \tfrac{1}{2}(\rho v^3)(\Delta n/n)^2. \qquad (2)$$

The light emerging from the sound wave interferes destructively except along certain directions. To find the direction of the diffracted light we return to Fig. 1 and construct wavefronts connecting points of the same phase. The light deflects into higher orders on each side of the

undeflected beam at an angle α for the qth order given by

$$\sin\alpha = \pm q(\lambda/\Lambda). \tag{3}$$

In practice α is very small so that $\alpha \cong \pm q(\lambda/\Lambda)$. For angles measured in air instead of in the medium in which the sound wave is generated, $\alpha \cong \pm q(\lambda_0/\Lambda)$ when the optical boundary of the medium is parallel to the sound beam.

The periodic variation of the phase of a wave is familiar in another context, namely FM systems. The sinusoidally varying index of refraction phase modulates the light wave at a frequency ω_s with the phase excursion or modulation index of $\Delta\phi$ given by Eq. (1). The carrier corresponds to the zero-order (undiffracted) light wave and the side bands at $\omega \pm \omega_s$, $\omega \pm 2\omega_s \cdots$ to the higher order diffracted light waves. The amplitude of the phase modulated light wave is

$$\begin{aligned} E &= E_s \exp(-i\omega t + i\Delta\phi \sin\omega_s t) \\ &= E_s \exp(-i\omega t) \sum_{q=-\infty}^{\infty} J_q(\Delta\phi) \exp(iq\omega_s t), \end{aligned} \tag{4}$$

where we have expanded in terms of ordinary Bessel functions $J_q(\Delta\phi)$.[15] Each higher order at frequency $\omega \pm q\omega_s$ has an intensity proportional to $J_q^2(\Delta\phi)$. The corresponding orders on each side of the undiffracted beam have equal intensity since $J_q^2(\Delta\phi) = J_{-q}^2(\Delta\phi)$. Figure 2 shows the relative intensity of light $J_q^2(\Delta\phi)$ in the first four orders. Notice that a traveling acoustic wave diffracts all of the light out of the zeroth order when $\Delta\phi = 2.4$ rad. Because of the sum rule,

$$J_0^2(\Delta\phi) + 2\sum_{q=1}^{\infty} J_q^2(\Delta\phi) = 1, \tag{5}$$

light diffracted out of one order must appear in another.[15]

So far we have considered light incident parallel to the acoustic wavefronts. In one of their later papers Raman and Nath[7] calculated the case of light incident obliquely at an angle θ to the acoustic wavefront. Then the intensity in order q was shown to be given by

$$I_q \propto J_q^2\left(\Delta\phi \sec\theta \frac{\sin(\pi W \tan\theta/\Lambda)}{\pi W \tan\theta/\Lambda}\right). \tag{6}$$

The diffraction pattern is symmetric at all angles of incidence, that is, $I_q = I_{-q}$ for all θ. Note also that the intensity of each order as a function of angle of incidence is symmetric about normal incidence, $\theta = 0$.

As mentioned previously, the above discussion applies to progressive ultrasonic waves. If the wave is reflected and standing waves are established, the situation is quite different. Twice each period the amplitude of the standing wave is zero everywhere and the ultrasonic grating is canceled. At these times all of the light is undiffracted and falls in the zero order so that it is never possible to completely eliminate the zero-order light. The total amount of light diffracted into higher orders is correspondingly smaller. The entire diffraction pattern is modulated with a frequency $2\omega_s$. Each order of light diffracted from standing waves contains numerous frequency components. The zero order and each even order have frequency components at all even harmonics ω, $\omega \pm 2\omega_s$, $\omega \pm 4\omega_s$, etc, while each odd order has frequency

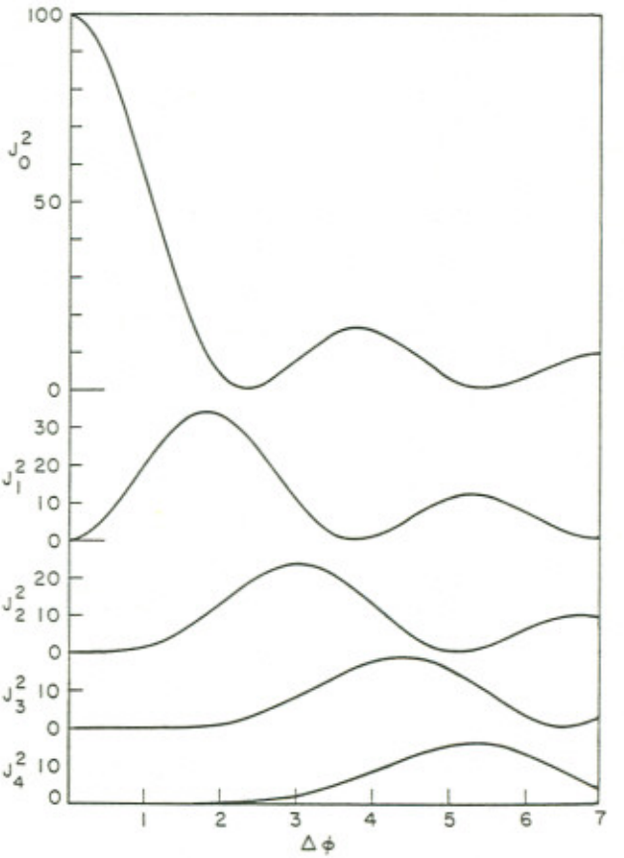

FIG. 2. The relative light intensity varies as $J_q^2(\Delta\phi)$ in the qth order for a phase change $\Delta\phi$ in the case of Raman–Nath diffraction from a progressive wave.

nponents at all odd harmonics $\omega \pm \omega_s$, $\omega \pm 3\omega_s$, $\pm 5\omega_s$, etc. The distribution of light intensity in e various orders is somewhat more complicated an in the case of diffraction from a progressive ave.[8]

The Raman–Nath theory described above is plicable when the curvature of the light beam wards regions of higher refractive index is gligible. The curvature can be negligible for everal reasons: (1) The variation in refractive index Δn is so small as to cause little curvature; (2) the width of the sound beam W is short enough so the integrated bending as the light traverses the sound beam is very small; or (3) the sound wavelength Λ is so long that the light can be bent some distance without passing through a region of significantly different Δn and hence the phase mismatch due to bending between the entering and emerging light ray is small. It is useful to have some criteria that takes account of these parameters and indicates the range of applicability of the Raman–Nath theory.

Lucus and Biquard[5] calculated the curvature of light rays incident from left to right and parallel to the acoustic wavefronts as shown in Fig. 3. The abscissa is the normalized distance into the sound beam $W' = 2\pi W(\Delta n/n)^{1/2}/\Lambda$. The light rays converge and first cross at $W' \cong \pi/2$. For W' near to and larger than $\pi/2$ the intensity distribution of the emerging light varies periodically along the sound beam with period Λ. Thus the sound wave acts as both a phase and an amplitude grating and the intensity in the diffracted orders is not

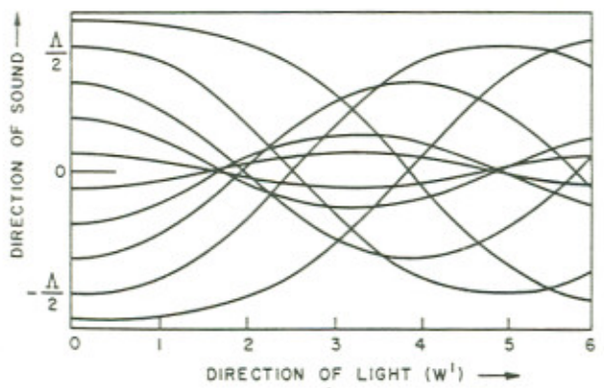

FIG. 3. Light incident from the left parallel to the acoustic wavefronts is bent toward regions of higher refractive index. The width of the sound column must be such that $W' < \pi/2$ from Raman–Nath diffraction (after Lucas and Biquard, Ref. 5).

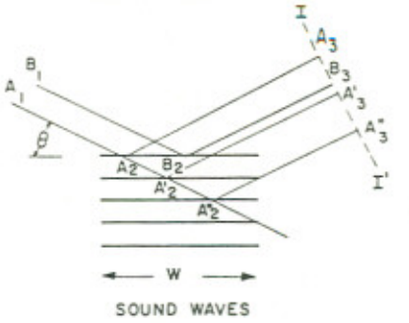

FIG. 4. For Bragg diffraction the incident and diffracted angles are equal, the pathlengths must be equal which requires $m\lambda = 2\Lambda \sin\theta$, and the sound column must be wide enough so that the light crosses at least two wavefronts.

given by Eq. (4). The amplitude grating effect becomes smaller as W' decreases below $\pi/2$. Willard[14] determined experimentally that diffraction measurements agree with the Raman–Nath theory within 10% when $W' \leqq \pi/2$. Thus the relation between W, Λ, and Δn for Raman–Nath diffraction is

$$W \leqq \tfrac{1}{4}\Lambda(n/\Delta n)^{1/2}$$

or

$$W \leqq (\Lambda^2/16)(n/\lambda)(2\pi/\Delta\phi). \qquad (7)$$

The criterion is somewhat arbitrary since there is no distinct line where suddenly the Raman–Nath theory becomes appropriate. Another criterion frequently used[16] ignores the sound intensity and considers only the phase mismatch caused by the diffraction of the light through the equivalent aperture $\Lambda/2$. The phase mismatch of the entering and emerging light due to the diffraction of the aperture is $4\pi W\lambda/\Lambda^2$. For the mismatch to be less than $\pi/4$ we have

$$W \leqq \Lambda^2/16\lambda, \qquad (8)$$

which is approximately equivalent to the previous criterion as long as $\Delta\phi < 2\pi$.

Both the amplitude and phase changes of the light are accounted for by a partial differential equation describing light propagation in a medium with sound waves. Raman and Nath obtained a set of coupled differential-difference equations that describe the general case. In the Raman–Nath region where Eq. (7) holds, the approximate

solution to these equations shows that the diffracted light has the expected Bessel function amplitudes. In the region where both amplitude grating and phase grating effects are important the general differential-difference equations no longer have simple analytic solutions. They have been solved numerically using a computer by Klein and Cook[17] to show the nature of the diffracted light in the transition region from Raman–Nath diffraction to Bragg diffraction.

B. Bragg Diffraction

When the sound beam is wide and the sound wavelength short, the diffracted light is a maximum when it is incident on the sound wave front at a particular angle. Also the diffracted light is in a *single* order on *one* side of the undiffracted beam. Figure 4 illustrates the physical reasons for this behavior.[14] Consider light rays $A_1A_2A_3$ and $B_1B_2B_3$ scattered from two points A_2 and B_2 on a given sound wave front. The light is in phase and interferes constructively at the plane II′ perpendicular to the reflected rays if the path lengths $A_1A_2A_3$ and $B_1B_2B_3$ are equal. The path lengths are equal if the incident and reflected angles are equal. Only some of the light scatters at the first wavefront. That light which scatters at equal angles from subsequent wavefronts at A_2' and A_2'' in Fig. 4 is in phase with light scattered at A_2 if the path lengths differ by an integral number of light wavelengths. Such constructive interference takes place at certain angles given by the Bragg relation

$$m\lambda = 2\Lambda \sin\theta. \tag{9}$$

The reinforcement from scattering at successive sound wavefronts, which is a criteria for Bragg diffraction, only occurs if the incident light ray passes through at least one entire sound wavelength. The more sound wavefronts N which the light ray crosses, the sharper and more intense is the diffracted light. Since the angles are small, we use the relation $\sin\theta = m\lambda/2\Lambda$ from the Bragg equation and $W\tan\theta = N\Lambda$ from Fig. 4 to give a minimum criteria for Bragg diffraction in the order m [15]

$$W \geqq 2N\Lambda^2/m\lambda, \tag{10}$$

where $N \geqq 1$. Here we refer to angles inside the medium with index of refraction n. The same Bragg condition holds if both the angle and light wavelength are measured in air. While no dependence on sound amplitude appears in the criteria of Eq. (10), Klein and Cook[17] have pointed out that true Bragg reflection also requires $\Delta\phi \ll 2\pi\lambda W/\Lambda^2 n$.

The frequency of the diffracted light ω_2 is Doppler shifted from the incident light frequency ω_1 by an amount equal to the sound frequency ω_s. The light diffracted from the oncoming sound waves toward the direction of sound propagation has an increased frequency while the light diffracted in the opposite direction from receding sound waves has a lower frequency. The Doppler shifted frequency ω_2 of the light diffracted through the angle 2θ from its initial direction is given by

$$\omega_2 = \omega_1[1 \pm 2(nv/c)\sin\theta], \tag{11}$$

and since $\sin\theta = m\lambda/2\Lambda$, we have $\omega_2 = \omega_1 \pm \omega_s$.

The diffraction process can be viewed in terms of quantized light and sound whereby an incoming photon collides with a phonon suffering a change in momentum and energy as illustrated by the

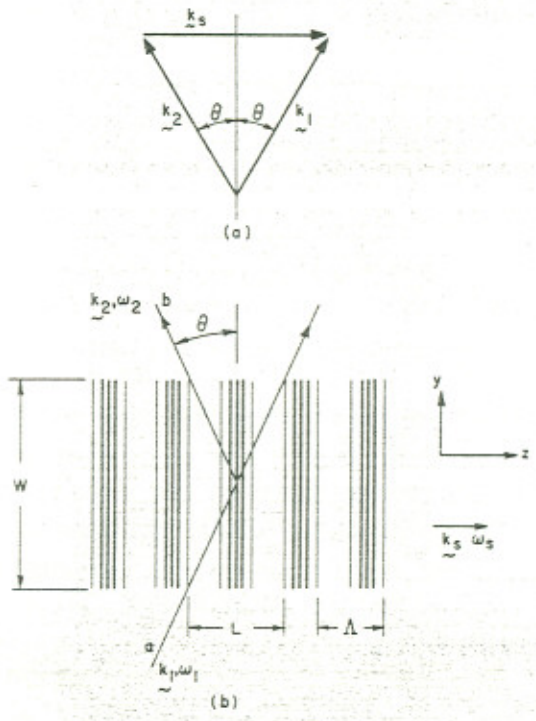

FIG. 5. (a) Momentum conservation diagram. (b) The Bragg diffraction configuration discussed in the calculation. The incident wave labeled a is at frequency ω_1 and the diffracted wave b is at $\omega_2 = \omega_1 - \omega_s$. The length of the interaction region is $L = W\tan\theta$.

vector diagram in Fig. 5(a). The conservation of energy and momentum provides the following relations:

$$\omega_1 = \omega_2 + \omega_s \tag{12}$$

and

$$\mathbf{k}_1 = \mathbf{k}_2 + \mathbf{k}_s, \tag{13}$$

which is equivalent to saying the frequency is Doppler shifted.

A powerful quantitative approach to this problem is to treat Bragg diffraction as a three-wave parametric interaction. We present this approach briefly following Quate *et al.*[12] The sound input ω_s interacts with the pump at ω_1 to produce the signal at $\omega_2 = \omega_1 + \omega_s$. Consider Fig. 5(b) where we show light waves with fields E_a (at ω_1) and E_b (at ω_2) both polarized in the x direction. The total field $E_x = E_a + E_b$ satisfies the wave equation

$$(\partial^2 E_x/\partial y^2) + (\partial^2 E_x/\partial z^2) = \mu(\partial^2 D_x/\partial t^2). \tag{14}$$

In the absence of sound the electric fields propagate as plane waves

$$E_a = \tfrac{1}{2}E_1 \exp[i(\omega_1 t - k_1 z \sin\theta - k_1 y \cos\theta)] + \text{c.c.}$$
$$= \tfrac{1}{2}E_1 \exp(i\phi_1) + \text{c.c.} \tag{15}$$

and

$$E_b = \tfrac{1}{2}E_2 \exp[i(\omega_2 t + k_2 z \sin\theta - k_2 y \cos\theta)] + \text{c.c.}$$
$$= \tfrac{1}{2}E_2 \exp(i\phi_2) + \text{c.c.} \tag{16}$$

The interaction takes place because the index of refraction of the medium is modulated by the change in density produced by the acoustic wave through the photoelastic effect. We assume that the intensity of the sound wave is unchanged by the interaction. For an acoustic wave giving rise to a periodic strain

$$S = \tfrac{1}{2}S \exp[i(\omega_s t - k_s z)] + \text{c.c.} = \tfrac{1}{2}S \exp[i\phi_s] + \text{c.c.}, \tag{17}$$

the change in the dielectric constant is given by

$$\Delta\epsilon/\epsilon = (-\epsilon/\epsilon_0)pS, \tag{18}$$

where p is the elasto-optical coefficient. In the case of a crystal p is a fourth-rank tensor relating different directions of strain and optical polarization.[18] Therefore, we have for the displacement

$$D = (\epsilon + \Delta\epsilon)(E_a + E_b). \tag{19}$$

Substituting the electric fields and strain wave into the wave equation one obtains a coupled set of equations

$$dE_1/dz = (ik_1 n^2 p/\sin\theta)(S/2)(E_2/2), \tag{20}$$

$$dE_2/dz = -(ik_2 n^2 p/\sin\theta)(S/2)(E_1/2). \tag{21}$$

In deriving these equations (which include their complex conjugates), we have assumed that E_1 and E_2 are slowly varying in the z direction so that d^2E/dz^2 is negligible. In addition, for cumulative interaction the frequency and wave vector of the source and driven terms must be the same. This requires $\phi_1 = \phi_2 + \phi_s$ which leads to the conservation conditions

$$\omega_1 = \omega_2 + \omega_s,$$
$$k_1 \sin\theta + k_2 \sin\theta = k_s,$$
$$k_1 \cos\theta = k_2 \cos\theta. \tag{22}$$

The amplitudes E_1 and E_2 of the waves vary in the z direction as $\exp(\pm\Gamma z)$ where

$$\Gamma = k_1 \left(\frac{\omega_2}{\omega_1}\right)^{1/2} \frac{\epsilon}{2\epsilon_0} \frac{p}{\sin\theta} \left(\frac{P_s}{2\rho v^2}\right)^{1/2}, \tag{23}$$

and $P_s = \tfrac{1}{2}\rho v^3 S^* S$ is the power density of the sound wave. The length of the interaction region is $L = W\tan\theta$. With the boundary conditions $E_2(L) = 0$ and $E_1(0) = E_1$, we find

$$E_1 = E_1(0)[\cosh\Gamma(z-L)/\cosh\Gamma L] \tag{24}$$

and

$$E_2 = -E_1(0)\left(\frac{\omega_1}{\omega_2}\right)^{1/2}\left(\frac{S^*}{S}\right)^{1/2} \frac{\sinh\Gamma(z-L)}{\cosh\Gamma L}. \tag{25}$$

The ratio of the diffracted power to the incident power is

$$P_2/P_1 = |E_2(0)/E_1(0)|^2 = (\omega_2/\omega_1)\tanh^2\Gamma L. \tag{26}$$

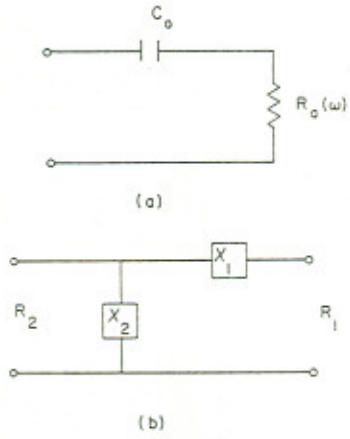

FIG. 6. (a) Electrical representation of the quartz crystal transducer. (b) L matching network.

For small ΓL, $\omega_1 \cong \omega_2$, and small θ this is approximately

$$P_2/P_1 = \tfrac{1}{2}\pi^2(n^6p^2/\rho v^3)\,(W^2P_s/\lambda_0^2), \qquad (27)$$

where the material parameters have been grouped in the parentheses. For sound waves in water $\rho = 1$, $v = 1.5 \times 10^5$ cm/sec, $n = 1.33$, and from the Lorentz–Lorenz relation $p \cong 0.31$. Since v can be determined from the Bragg equation, it is possible to determine p from Eq. (27). For a crystal, of course, p would have different values depending on the crystal orientation. The elasto-optic coefficient p has been measured for a variety of materials.[19–21]

A special case of Bragg diffraction occurs for three waves propagating collinearly. At the correct sound frequency phase matching is guaranteed by the collinearity and a long interaction length can be obtained. In an anisotropic crystal Bragg scattering may lead to a change in polarization, a feature which has important practical applications as discussed in Sec. IV.

III. EXPERIMENT

The basic equipment for this experiment is not elaborate and is probably available in most laboratories. A conveneient light source is a 1–5 mW He–Ne laser. However, a Hg lamp or white light source with appropriate optics to condense and collimate the light may be used.

An amateur radio transmitter works well as an rf power source. We used a Viking Challenger transmitter, somewhat off its rated operating frequency, to drive the fundamental and odd harmonics of the 5 MHz X-cut quartz crystal.[22] Ideally one would select the crystal frequency most compatible with the rf source.

Figure 6(a) shows an electrical representation of the acoustic tranducer. The capacitance C_0 is the transducer capacitance and R_a is the real part of the impedance which represents acoustic power flow into the medium. The problem of impedance matching the acoustic transducer is treated in detail by Reeder and Winslow[23] and is outlined in the Appendix. For a quartz transducer in water, the effective impedance to be matched is typically 1 kΩ so that series-parallel capacitance or inductance elements are required as shown in Fig. 6(b).

The easily constructed aluminum or brass rectangular tank shown in Fig. 7 served as the water tank. Microscope slides make suitable cell windows. They are cemented with waterproof epoxy or RTV rubber cement. The transducer is fastened on the end of the cell with heavy grease or with RTV cement. The grease is suitable as long as it is not heated by high sound power. Electrical contact is made directly to each electrode or via the water to the inner electrode. An acoustic absorber such as a piece of Lucite is placed at the end of the tank. The attenuation of water is high enough that for a tank 15 cm long the reflected wave in the light–sound interaction region is small.

In later experiments we immersed the transducer in the water to avoid making the waterproof grease seal. The water's electrical resistance is high enough at 5, 15, and 25 MHz that bare electrical leads could be used to make contact with the transducer. This configuration simplifies

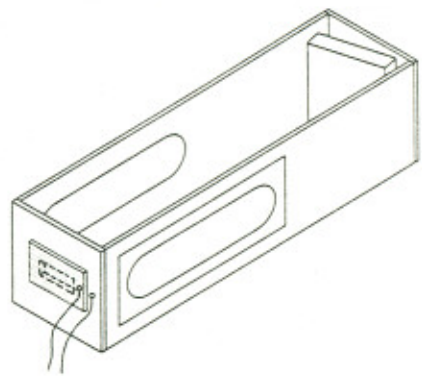

FIG. 7. A suitable water tank for observing generated sound waves.

onstruction of the box and simultaneously provides cooling for the transducer.

The equipment described thus far is sufficient to observe both Raman–Nath and Bragg diffracted light spots on a screen. To obtain a quantitative measure of the incident and diffracted light, we used inexpensive silicon detectors. The rotating mirror in the setup of Fig. 8 conveniently displays the intensity of the Raman–Nath diffracted orders on the oscilloscope. A plane mirror attached to the shaft of a synchronous motor (400 rpm for example) reflects the light to detector 1 which triggers the oscilloscope and then to detector 2 which measures the light intensity which is then displayed on the oscilloscope. The correct trigger delay is provided by adjusting the position of detector 1. This rotating mirror system also gives a convenient measure of the laser beam diameter and Gaussian intensity profile.

With a 1 cm wide acoustic beam in water and 6328 Å light, the acoustic frequency range from 5 to 45 MHz spans the range from Raman–Nath to Bragg diffraction. At 5 MHz we find from Eq. (7) that for Raman–Nath diffraction W should be less than 1.2 cm for a large $\Delta\phi = 2\pi$. At 35 MHz we find from Eq. (8) for first-order Bragg diffraction and $N = 1$ that W should be greater than 0.6 cm. Diffraction more solidly in the Raman–Nath regime is obtained by decreasing the sound beam aperture to 0.5 cm, and diffraction more solidly in the Bragg regime is obtained by

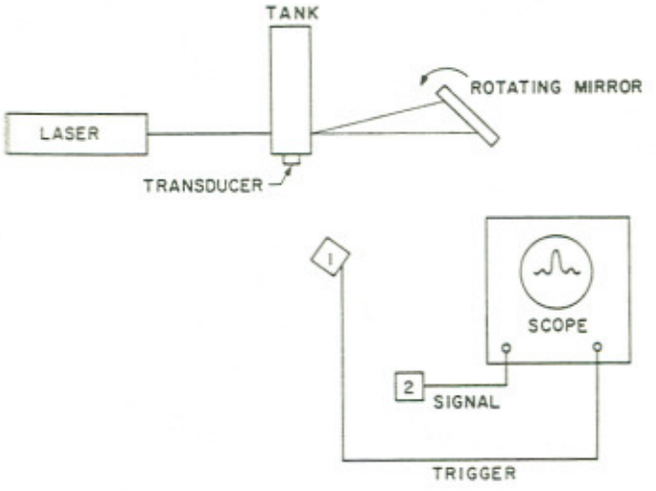

FIG. 8. Schematic diagram of experimental system for observing the intensity of several orders of Raman–Nath diffraction.

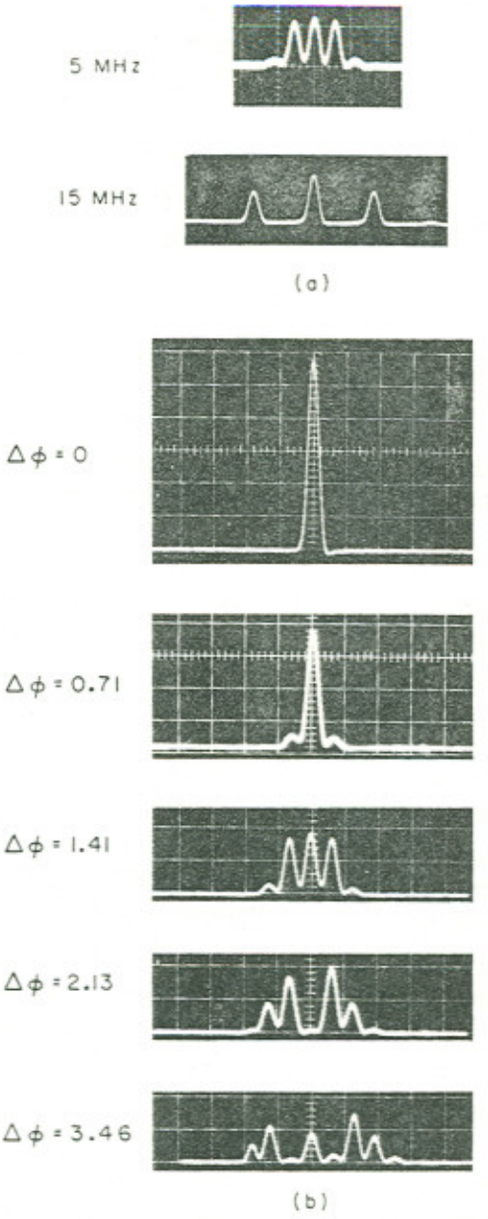

FIG. 9. Results of two experiments investigating Raman–Nath diffraction in the student laboratory. (a) Dependence of the angle of the diffracted light on frequency is shown by the position of the first order peaks relative to the zero order in the scope traces. (b) Typical intensity distributions observed in diffracted spectra for a range of $\Delta\phi$.

increasing the width of the aperture. Frequencies of 15 and 25 Hz lie in an intermediate region where a single Bragg diffracted order is not produced. Multiple spots are produced on either side of center and do not appear and disappear symmetrically with incident angle as would be expected for pure Raman–Nath diffraction.

It is quite exciting to see several Raman–Nath diffracted orders. The measured angles of the

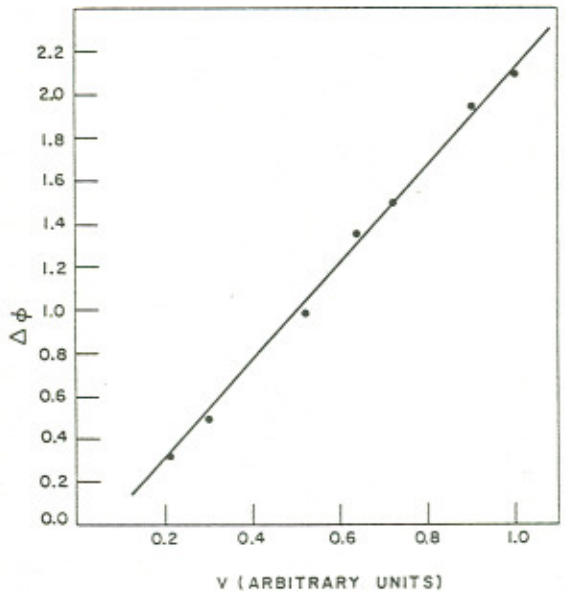

FIG. 10. Results of a third experiment showing the relation between $\Delta\phi$ and the voltage applied to the transducer. Only relative voltage measurements were obtained.

diffracted light beams and Eq. (3) allow us to determine the sound velocity since ω_s and λ are known. In Fig. (9) we give examples of the intensity distribution displayed on the oscilloscope. Figure 9(a) compares oscilloscope traces of the diffracted orders at 5 and 15 MHz where care was taken to maintain the detectors in the same position. The first-order diffraction at 15 MHz occurs at an angle three times as large as for 5 MHz and the first-order peak is correspondingly displaced on the scope trace. The oscilloscope traces of Fig. 9(b) show a wide range of $\Delta\phi$ from 0 to 3.46 as determined approximately from Fig. 2. The slight asymmetry in the orders may be due to the light not being exactly parallel to the sound wavefronts or due to distortions in the sound wave. We measured the relative sound power applied to the transducer by measuring the rf voltage. This is conveniently done with the oscilloscope, or with a small pickup loop and diode in the vicinity of the experiment attached to an ammeter. Although only a relative voltage measurement is obtained, it is sufficient to show the relation of $\Delta\phi$ and V as displayed in Fig. 10. The linear relation between $\Delta\phi$ and V is expected from Eq. (2) since P_s is proportional to V^2.

We measured the difference in frequency of the diffracted and undiffracted light by observing the beat frequency resulting when the two orders interfered on a fast detector.[24] The efficiency of this optical heterodyning is very sensitive to alignment and care must be taken so that the two light beams are collinear when they impinge on the detector.[25] Photomultiplier tubes or silicon detectors are fast enough to measure the 5–15 MHz signal. The beat signal should disappear if either the diffracted or undiffracted beam is blocked. Note that if any stationary sound waves are present a diffracted beam contains higher harmonics, and the single beam can give rise to a beat signal.

By increasing the sound frequency or width of the acoustic column, Raman–Nath diffraction changes to the Bragg diffraction where a single order is observed at the Bragg angle given by Eq. (9). In our experiment we increased the frequency by exciting higher odd harmonics of the 5 MHz transducer. Equation (27) states that the diffraction efficiency is proportional to the sound power. We verified this dependence by monitoring the acoustic power intensity as explained above.

Bragg diffraction is a powerful nondestructive method for measuring material properties. As seen from Eq. (27), a measurement of diffraction efficiency and sound power determines the elasto-optic coefficient. Bragg diffraction has been used extensively to determine the elasto-optic coefficients of crystals for acoustic beams at various orientations to the crystal axes.[20,21] In addition, the velocity of sound in the medium and the acoustic attentuation can be measured. In this experiment we measured the attenuation coefficient of water by simply measuring the diffraction efficiency P_2/P_1 as a function of the distance from the driving transducer. In a similar manner, acoustic attenuation vs frequency can be measured.

While many of the interesting applications of Bragg diffraction involve the use of crystals and higher acoustic frequencies, at least one application of interest uses Bragg diffraction from acoustic waves in water as in this laboratory experiment. If an object such as a fish lies in a sound beam, the change in intensity across the sound beam corresponds to the density variation of the interrupting object. The Bragg diffracted light from the modified acoustic wavefront can be imaged with lenses to give an optical representation of the object in the acoustic beam; the fish

for example. We discuss briefly more applications of the interaction of light and sound in Sec. IV.

IV. APPLICATIONS

This laboratory experiment illustrates the basic phenomena of the interaction of light and sound. In this section we discuss briefly a few applications of these phenomena—light beam scanning, light modulation, monochromatic filtering, and acoustic imaging. These applications also suggest ways in which this laboratory experiment could be extended.

Bragg diffraction scanning of a light beam has potential applications in television and for memory devices. From Eq. (9) we know that the sine of the Bragg angle is proportional to the sound frequency. The light beam can be scanned by varying the sound frequency. The usefulness of this technique depends on the number of resolvable spots. The light beam of width D has an angular spread due to diffraction of λ/D. For small angles the variation in the Bragg angle is $\Delta(2\theta)=\Delta\omega_s\lambda/\omega_s\Lambda$. The ratio of the variation in Bragg angle to the minimum beam divergence gives the number of resolvable spots as $(\Delta\omega_s/\omega_s)(D/\Lambda)$. Practical light deflectors require a wideband $(\Delta\omega_s/\omega_s\sim 0.2)$ and transducers that operate at high frequencies to achieve even 100 resolvable spots.

Either Raman–Nath or Bragg diffraction can modulate light beams. A variable acoustic intensity produced by modulating the rf voltage applied to the transducer produces the desired modulation. Recently Korpel *et al.*[26] described an experimental television display using acoustic deflection to modulate a coherent light beam. In the experiment light from a He–Ne laser was modulated with the video signal by Bragg diffraction in a water cell at 43 MHz.

Some of the more exotic applications of the acoustic diffraction of light occur in anisotropic crystals where the acoustic interaction rotates the diffracted light polarization. For such cases the equations for Bragg diffraction require modification.[27] Harris and Wallace[28] describe an electronically tunable optical filter which makes use of collinear diffraction in an optically anisotropic crystal. Of the white light incident on the crystal, only a small range of optical frequencies satisfies the momentum matching requirement and diffracts to the correct polarization to provide a narrow band filter. The band of optical frequencies tunes by varying the acoustic frequency.

The intensity distribution across a sound beam can be explored using Bragg diffraction. The change in diffracted light intensity as a function of the incident angle θ is the Fourier transform of the acoustic intensity across the beam.[29] It is possible to image the diffracted light and obtain an image of an object placed in the acoustic beam.[30] This is the principle of the acoustic microscope. The resolution of the acoustic microscope is theoretically comparable an optical microscope since $\Lambda\approx\lambda$ at 10^9 Hz acoustic frequency. The acoustic microscope's advantages are that specimens can be studied *in vivo* and it is sensitive to density changes rather than small index of refraction changes as in an optical microscope.

APPENDIX: IMPEDANCE MATCHING

To maximize the acoustic output of a transducer it is necessary to impedance match a 50 Ω source into the transducer. This problem is treated in detail by Reeder and Winslow.[23] This Appendix discusses the more direct problem of matching into a resonant transducer of arbitrary impedance.

Figure 6(a) shows an equivalent circuit of the acoustic transducer. The capacitance is

$$C_0=\epsilon\epsilon_0 A/t, \tag{A1}$$

where ϵ is the dielectric constant, A the area, and t the thickness. If the transducer is excited on resonance the electrical input impedance has the form

$$Z=(1/j\omega_0 C_0)+Z_a, \tag{A2}$$

where ω is the excitation frequency and

$$Z_a=R_a+jX_a \tag{A3}$$

is the radiation impedance resulting from acoustic excitation. On resonance Reeder and Winslow show that

$$R_a=(4k^2/\pi)(Z_T'/Z_L')(\omega_0 C_0)^{-1}(\omega_0/\omega)^2$$

and

$$X_a=0, \tag{A4}$$

where k is the electromechanical coupling constant, Z_T' is the specific acoustic impedance of the transducer, and Z_L' is the specific acoustic impedance of the acoustic medium being excited. $Z'=\rho v$ and has the units kilogram per square meter second in the mks system. For example, the acoustic impedance of water is $Z_L'=1.5\times10^6$ while that for an X-cut longitudinal quartz transducer is $Z_T'=13.3\times10^6$. The electromechanical coupling constant for the above quartz transducer is $k_{11}=0.093$. The velocity of sound in the transducer is 5×10^5 cm/sec so that the $\Lambda/2$ thickness for a 5 MHz resonant frequency is 0.5 mm. Our particular transducer was 0.4×2.0 cm area with $\epsilon/\epsilon_0=4.5$ so that $C_0=6.3$ pF.

Using the above values, the real part of the impedance is calculated to be $R_a=50\ \Omega$ at 5 MHz. This transducer was cut by the manufacturer to provide proper impedance matching to water at 5 MHz. At 15 MHz the impedance decreases to 5.5 Ω thus necessitating impedance matching for maximum power transfer.

The problem of impedance matching by an L network of the type shown in Fig. 6(b) leads to impedance values

$$X_2=\pm R_2[R_1/(R_2-R_1)]^{1/2} \qquad \text{(A5)}$$

and

$$X_1=\mp[R_1(R_2-R_1)]^{1/2} \qquad \text{(A6)}$$

for $R_2>R_1$ at the matched condition. The impedances X_2 or X_1 include the capacitance of the transducer. The impedance $Z_2=jX_2$ or $Z_1=jX_1$ may be either inductance or capacitance. Experimentally we find slightly better matching using inductance.

If the transducer impedance is greater than 50 Ω, then

$$X_2'=X^2/(1+X_2\omega C_0), \qquad \text{(A7)}$$

and if the tranducer impedance is less than 50 Ω, then

$$X_1'=(\omega C_0)^{-1}\mp[R_1(R_2-R_1)]^{1/2}, \qquad \text{(A8)}$$

where X_2' and X_1' are the additional impedance necessary to properly match the transducer to the input impedance.

For our example at 15 MHz, $1/\omega C_0=1680\ \Omega$ and $R_1=5.5\ \Omega$. For inductive matching we find $\omega L_1'=1665\ \Omega$ or $L_1'=16.7\ \mu$H and $L_2'=0.186\ \mu$H.

Experimentally it is straightforward to choose an air core coil of proper inductance and match by tapping at the proper turns ratio. At 5 MHz a series inductance is required to match the 6.3 pF transducer capacitance. From Eq. (A8) the inductor has a value $L=1/\omega^2C_0=6.36$ mH. We use a small adjustable inductor to achieve optimum matching.

ACKNOWLEDGMENTS

The authors have benefited from discussions with T. H. DiStefano, J. F. Havlice, M. D. Levenson, J. M. Murray, and D. C. Wolkerstorfer as well as from other colleagues at Stanford and the students participating in the laboratory.

* Present address: Laboratorium für Festokörperphysik, Eidgenössische Technische Hochschule, Hönggerberg, CH-8049 Zürich, Switzerland.

[1] L. Brillouin, Ann. Phys. (France) **7**, 88 (1922).
[2] E. H. Jacobsen, Rev. Mod. Phys. **30**, 234 (1958).
[3] J. Laval, Rev. Mod. Phys. **30**, 222 (1958).
[4] P. Debye and F. W. Sears, Proc. Nat. Acad. Sci. (USA) **18**, 409 (1932).
[5] R. Lucas and P. Biquard, J. Phys. Rad. **3**, 464 (1932).
[6] C. V. Raman and N. S. Nagendra Nath, Proc. Indian Acad. Sci. **2**, 406 (1935).
[7] C. V. Raman and N. S. Nagendra Nath, Proc. Indian Acad. Sci. **2**, 413 (1935).
[8] C. V. Raman and N. S. Nagendra Nath, Proc. Indian Acad. Sci. **3**, 75 (1936).
[9] C. V. Raman and N. S. Nagendra Nath, Proc. Indian Acad. Sci. **3**, 119 (1936).
[10] C. V. Raman and N. S. Nagendra Nath, Proc. Indian Acad. Sci. **3**, 459 (1936).
[11] The diffraction of light by sound has been treated in many texts including L. Bergmann, *Ultrasonics*, translated by H. S. Hatfield (Wiley, New York, 1938); and M. Born and E. Wolf, *Principles of Optics* (Pergamon, New York, 1959).
[12] C. F. Quate, C. D. W. Wilkinson, and D. K. Winslow Proc. IEEE **53**, 1604 (1965).
[13] P. Kang and F. C. Young, Amer. J. Phys. **40**, 697 (1972).
[14] G. W. Willard, J. Acoust. Soc. Amer. **21**, 101 (1949).
[15] G. N. Watson, *Theory of Bessel Functions* (MacMillan, New York, 1944).
[16] R. Adler, IEEE Spectrum **4**, 42 (1967).
[17] W. R. Klein and B. D. Cook, IEEE Trans. Sonics Ultrasonics **14**, 123 (1967).
[18] J. F. Nye, *Physical Properties of Crystals* (Oxford U. P., Oxford, England, 1957), Chap. 13.

[19] V. Raman and K. S. Venkataraman, Proc. Roy. Soc. (London) **171**, 137 (1939).
[20] T. M. Smith and A. Korpel, IEEE J. Quantum Elec. 1, 283 (1965).
[21] R. W. Dixon, J. Appl. Phys. **38**, 5149 (1967).
[22] Sources of crystals include Valpey Corporation, Holliston, Mass.
[23] T. M. Reeder and D. K. Winslow, IEEE Trans. Microwave Theory Techniques **MTT-17**, 927 (1969).
[24] H. Cummins, N. Knable, L. Gampel, and Y. Yeh, Appl. Phys. Lett. **2**, 62 (1963).
[25] A. E. Siegman, Appl. Opt. **5**, 1588 (1966).
[26] A. Korpel, R. Adler, P. Desmares, and W. Watson, Proc. IEEE **54**, 1429 (1966).
[27] R. W. Dixon, J. Quantum Elec. **3**, 85 (1967).
[28] S. E. Harris and R. W. Wallace, J. Opt. Soc. Amer. **59**, 744 (1969).
[29] M. G. Chen and E. I. Gordon, Bell System Tech. J. **44**, 693 (1965).
[30] A. Korpel, Appl. Phys. Lett. **9**, 425 (1966).

The Concept of Temperature in Magnetism

N. BLOEMBERGEN
Division of Engineering and Applied Physics
Harvard University
Cambridge, Massachusetts 02138
(Received 1 August 1972)

This is an English translation of a paper which appeared in Nederlands Tydschrift voor Natuurkunde, [**38**, *198 (1972)*] *in honor of H. B. G. Casimir.*

I. INTRODUCTION

In the 1930's the question of how a magnetic system attains thermal equilibrium received much attention. This interest was stimulated by the early experiments in adiabatic demagnetization and in magnetic relaxation. The early history and development of the field of paramagnetic relaxation until the end of World War II has been reviewed in a monograph by Gorter.[1] An important concept in the interpretation of spin–lattice relaxation phenomena was provided by the thermodynamic theory of Casimir and DuPré.[2] They considered the magnetic crystal to be composed of two systems which could be assigned two different temperatures. One system contained the magnetic degrees of freedom. This magnetic system was supposed to come into internal equilibrium at temperature T_M in a very short time. This spin–spin relaxation time is denoted by t_{ss} or T_2. The other system, called the lattice, contains all other degrees of freedom, phonons, translational motion of conduction electrons, etc. It is at a temperature T_L which may be different from T_M. The time necessary to establish thermal equilibrium between the two systems is called the spin–lattice relaxation time, t_{ML} or T_1. For a typical magnetic material, iron alum at 4°K, one has $t_{ML} \sim 10^{-3}$ sec, while $t_{ss} \sim 10^{-10}$ sec. The notion of two different temperatures is useful if we look at a phenomena with a characteristic time scale between these two times.